

Techno-economic comparison of various process configurations for post-combustion carbon capture using a single-component water-lean solvent

Yuan Jiang ^a, Paul M. Mathias ^{b,*}, Charles J. Freeman ^a, Joseph A. Swisher ^c, Richard F. Zheng ^a, Greg A. Whyatt ^a, David J. Heldebrant ^{a,d,*}

^a Pacific Northwest National Laboratory, Richland, WA, 99352, USA

^b Fluor Corporation, Aliso Viejo, CA, 92656, USA

^c Electric Power Research Institute, Palo Alto, CA, 94304, USA

^d Department of Chemical Engineering, Washington State University, Pullman, WA 99164



ARTICLE INFO

Keywords:

Post-Combustion CO₂ capture
Water-lean solvent
Process configurations
Process modeling
Techno-Economic analysis

ABSTRACT

Aqueous amines-based absorption is the most mature and scalable technology for post-combustion carbon capture, but subject to high energy and capital investment costs. Water-lean solvents, with associated advanced process configurations, show promise of significantly reducing both energy and capital costs via lower solvent recirculation and lower water condensation and vaporization. Even though advanced process configurations have been intensively studied for aqueous amines, few discussions can be found in the open literature for water-lean solvents. In order to fill the gap, the present study focuses on the process designs towards lower carbon capture cost enabled by water-lean solvents. N-(2-ethoxyethyl)-3-morpholinopropan-1-amine (EEMPA), a single-component water-lean solvent, was selected as an archetypical water-lean solvent. A property package was developed for the H₂O–CO₂-EEMPA system based on experimental data. Process models were developed in Aspen Plus for 90% CO₂ capture in a 550 MW supercritical pulverized coal power plant, with optimal operating conditions determined by sensitivity studies. Techno-economic analyses were performed to compare seven process configurations: simple stripper, two-stage flash, lean vapor compression, inter-heated column, advanced flash stripper, low-pressure steam heater, and advanced heat integration. The results show a two-stage flash configuration, has a carbon capture cost of \$47.1/tonne CO₂ (in 2011 US dollars), about 19% lower than the industrial benchmark, Cansolv. While considerable capture cost reductions have been proven for aqueous amine using lean vapor compressor and advanced flash stripper, those configurations were shown to have negligible impacts with water-lean solvents due to differences in solvent's physical properties.

1. Introduction

Electricity production is one of the largest sources of anthropogenic greenhouse gases (GHG), contributing to roughly 27% of the total U.S. GHG emissions, and 25% of the total global GHG emissions (EPA, 2020). Due to the concern of global warming, development of CO₂ capture technologies has gained increasing interest as an effective way to reduce GHG emissions without decreasing energy demands (Zhang et al., 2016; Van Wagener and Rochelle, 2011; Xue et al., 2017; Bui et al., 2018). Among technologies under development, aqueous amine-based absorption is one of the most mature and scalable options for

post-combustion CO₂ capture and sequestration (CCS) (Van Wagener and Rochelle, 2011a). However, the high energy penalties and the necessary capital investments limit its economic viability and widespread implementation (NETL, 2015; Stowe and Hwang, 2017). As shown in Fig. 1, for aqueous amine systems, energy penalties, mainly from reboiler heat rate, contribute to more than half of the total carbon capture cost, where heat of vaporization dominates almost one-third of the total energy penalties (NETL, 2010; Jiang et al., 2019a, b; Sakwatanapong et al., 2005). Several studies have proved that these energy penalties, particularly the heat of vaporization, can be significantly reduced by either replacing aqueous amine with water-lean solvents (Mathias et al., 2013; Zheng et al., 2020) or utilizing advanced

* Corresponding authors.

E-mail addresses: paul.m.mathias@fluor.com (P.M. Mathias), david.heldebrant@pnnl.gov (D.J. Heldebrant).

Nomenclature			
AACE	Association for the Advancement of Cost Engineering	PTx	Pressure-Temperature-Liquid Composition
AFS	Advanced flash stripper	PZ	Piperazine
AHI	Advanced heat integration	SS	Simple stripper
AP	Aspen Plus	ST	Steam turbine
APEA	Aspen Process Economic Analyzer	T&S	Transportation and storage
ASTM	American	TEA	Techno-economic analysis
CCC	Carbon capture and compression	TSF	Two-stage flash
CCS	CO ₂ capture and sequestration	VLE	Vapor-liquid equilibrium
CEPCI	Chemical Engineering Plant Cost Index	WWC	Wetted-wall column
CO ₂ BOLs	CO ₂ -binding organic liquids		
COE	Cost of electricity		
CW	Cooling water		
DCC	Direct contact cooler		
DOE	Department of Energy		
EDR	Exchanger design and rating		
EEMPA	N-(2-ethoxyethyl)-3-morpholinopropan-1-amine		
ENRTL-RK	Electrolyte non-random two liquid model with Redlich-Kwong		
GHG	Greenhouse gas		
HHV	Higher heating value		
HP	High pressure		
IHC	Interheated column		
LL	Lean loading		
LP	Low pressure		
LPH	Low-pressure steam heating		
LVC	Lean vapor compressor		
MEA	Monoethanolamine		
MOC	Material of construction		
MPS	Multi-pressure stripper		
MSF	Multi-stage flash		
NETL	National Energy Technology Laboratory		
PC	Pulverized coal		
PNNL	Pacific Northwest National Laboratory		
PR	Pressure ratio		

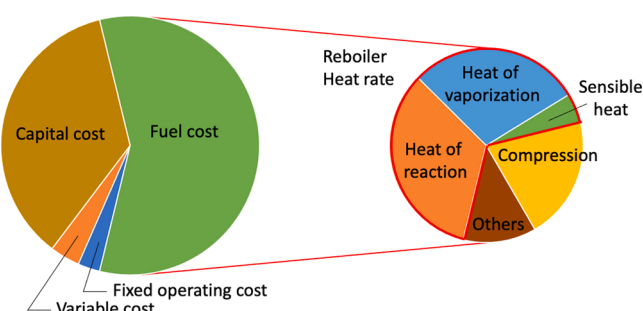


Fig. 1. Cost breakdown of post-combustion carbon capture using 30 wt% aqueous MEA.

configurations for solvent regeneration (Van Wagener and Rochelle, 2011). However, these studies focus on aqueous amines. This study provides the first comprehensive techno-economic comparisons of seven different configurations for absorption-based post-combustion carbon capture process using an archetypical water-lean solvent and assess different process variables with the aim of further lowering the total carbon capture cost.

In the past few years, water-lean solvents have been explored as alternatives to aqueous amines (Heldrebrand et al., 2014, 2017; Lail et al., 2014), with the goal of reducing recirculation rates and condensation/

PTx	Pressure-Temperature-Liquid Composition
PZ	Piperazine
SS	Simple stripper
ST	Steam turbine
T&S	Transportation and storage
TEA	Techno-economic analysis
TSF	Two-stage flash
VLE	Vapor-liquid equilibrium
WWC	Wetted-wall column
<i>Roman symbols</i>	
a	Activity [mol/L]
A_i, B_i, C_i, E_i	Model parameters
C_p	Heat capacity [kJ/kg/K]
C_{Tot}	Solution molarity [kmol/m ³]
E_i	Activation Energy [J/mol]
ΔH_s	Heat of solution [kJ/mol CO ₂]
K_G	Total mass transfer coefficient [mol/s/m ² /Pa]
k_{i0}	Pre-exponential kinetic parameter
K_{eq}	Chemical equilibrium constant
\dot{m}	Mass flowrate [kg/hr]
T	Temperature [K]
P	Pressure [kPa]
R	Gas constant [J/mol/K]
R_i	Reaction rate [kmol/m ³ /hr]
Q_r	Solvent regeneration heat rate [kJ/mol CO ₂]
V_{ca}	Parameters in the density model
w	Weight fraction
W_{net}	Net power output [MW]
W_{Total}	Total equivalent work for carbon capture [kJ _e /mol CO ₂]
<i>Greek symbols</i>	
α_{CO_2}	CO ₂ loading [mol CO ₂ /mol solvent]
β, γ	Model parameters
η	Efficiency [%]
μ	Viscosity [cP]

vaporization of water in the system, which can potentially lower both energy and capital costs. Many studies have suggested transformative improvements in lowering energy penalties. However, the majority of these water-lean solvent systems still remain at low technology readiness level and are inhibited from progressing due to the lack of property measurements required for rigorous process modeling and design for large-scale performance projections. CO₂-binding organic liquids (CO₂-BOLs) are a class of water-lean solvents developed at Pacific Northwest National Laboratory (PNNL) that represents an extensive library of chemical structures, formulations, and comprehensive property measures for several specific solvent types (Mathias et al., 2013; Whyatt et al., 2016; Cantu et al., 2020; Zheng et al., 2016; 2020). Among the well-characterized CO₂BOL derivatives, N-(2-ethoxyethyl)-3-morpholinopropan-1-amine (EEMPA) (Zheng et al., 2020; Cantu et al., 2020), as illustrated in Fig. 2 (1) retains “water-lean” functionality for low energy penalties as a single-constituent solvent (instead of a blend), (2) overcomes past viscosity challenges observed in other CO₂BOL derivatives (Mathias et al., 2013), and (3) can be made at

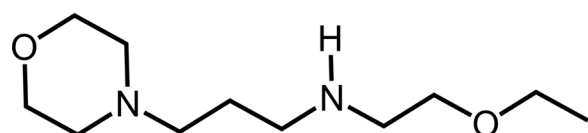


Fig. 2. Chemical structure of EEMPA.

an economical price via a single-step synthesis (Zheng et al., 2020). Due to these superior characteristics and supported by the availability of physical and thermodynamic property data, EEMPA is selected as an archetypical solvent to demonstrate the potential reduction of carbon capture cost enabled by the development of water-lean solvents and the optimization of process configurations.

In addition of the attributes of the solvent itself, carbon capture costs can also be reduced by the development of advanced processing configurations (Amrollahi et al., 2011; Van Wagener and Rochelle, 2011a, 2011b). Amrollahi et al. conducted exergy analysis of several chemical absorption carbon capture configurations and suggested that the total work demands can be reduced by 11.5% by lean vapor compression and absorber inter-cooling (Amrollahi et al., 2011). Van Wagener and Rochelle (2011a; 2011b) compared five different configurations of solvent regeneration for aqueous monoethanolamine (MEA) and piperazine (PZ) systems at their optimal lean loadings, including simple stripper (SS), multi-stage heated flash (MSF), lean vapor compressor (LVC), inter-heated column (IHC), multi-pressure stripper (MPS). The results indicated that all those advanced configurations have the potential to reduce energy penalties, of which IHC is the best, providing about 5% lower energy penalty than the standard SS configuration (Van Wagener and Rochelle, 2011a). Lin and Rochelle (2014) proposed advanced flash stripper (AFS) as a new configuration for solvent regeneration, which could provide about 10% energy saving and 15% cost savings compared to SS for CO₂ capture using aqueous PZ. LVC, on the other hand, is the configuration selected by technology vendors for both Fluor's Econamine FG PlusSM system (Scherffius et al., 2013) and Shell's Cansolv system (NETL, 2015), the benchmark solvents recommended by National Energy Technology Laboratory (NETL) of the U.S. Department of Energy (DOE) for post-combustion carbon capture (NETL, 2010, 2015). Similar work has also been conducted by other research groups (Ahn et al., 2013) for aqueous amine systems, all suggesting cost and energy savings are possible with advanced configurations and process optimizations. However, to the best of this authors' knowledge, the potential energetic benefits of advanced process configurations haven't been analyzed for water-lean solvents using rigorous process models based on high-quality thermodynamic data. Due to considerable differences in water loading, physical and thermodynamic properties between aqueous and water-lean solvents, viable configurations and operating conditions for aqueous amine systems may not be the optimal for water-lean solvents (Zheng et al., 2020). Re-evaluating those possible configurations for water-lean solvents is of crucial importance to further reduce the carbon capture cost. Thus, there is a need to integrate the energetic and cost benefits of water-lean solvents and advanced process configurations.

Process modeling and techno-economic analyses (TEAs) are widely

used to compare and optimize different carbon capture technologies in terms of net plant efficiency, total equivalent work, cost of electricity, and carbon capture cost (NETL, 2010, 2015; Van Wagener and Rochelle, 2011a). However, differences in economic and model assumptions as well as uncertainties in property model and capital cost estimation may significantly impact the performance and cost projections (Jiang et al., 2019a, b; Mathias and Gilmartin, 2014, 2020). To address these concerns, Monte Carlo simulations can be used to quantify the uncertainties in TEA from system-level economic assumptions and plant performance measures (Jiang et al., 2019a, b); methods including Monte Carlo sampling (Jones et al., 2019), Bayesian inference (Morgan et al., 2020) and perturbation scheme analysis (Mathias and Gilmartin, 2014, 2020) are being applied to quantify the uncertainties from property models, which are fundamental to all process models. However, if using a rigorous approach, uncertainty quantifications in both system-level analysis and property models can be computationally, mathematically, and data intensive. Among the above methods, the perturbation scheme analysis proposed by Mathias and Gilmartin (2014; 2020), focusing on uncertainties from physical quantities rather than parameters in property models, offers the simplest approach with lowest data requirement to include property model-related uncertainties into a primary TEA.

With the above serving as motivations, primary techno-economic analyses with perturbation were conducted to compare seven different configurations for post-combustion carbon capture using EEMPA. The key process and economic measures include heat rate for solvent regeneration, equivalent work for carbon capture, net plant efficiency of the power plant with CCS, total plant cost of CCS and the carbon capture cost. The contributions of this work can be summarized as follows: (1) develop and validate a primary thermodynamic package for the EEMPA-H₂O-CO₂ system based on experimental data collected at typical operating conditions (Zhang et al., 2020); (2) design and simulate commercial scale EEMPA-based carbon capture plants with seven configurations, including SS, two-stage flash (TSF), LVC, IHC, low-pressure steam heating (LPH), AFS, and advanced heat integration (AHI); (3) recommend optimal lean loading and regeneration pressure for EEMPA system based on sensitivity studies; and (4) conduct primary techno-economic comparison between the seven configurations at the optimistic, baseline, and conservative schemes.

2. Methods

In this study, process models are developed using Aspen Plus V10 for the entire supercritical pulverized coal (PC) Rankine cycle power plant with CCS. The most widely used approaches suggested in open literature (NETL, 2015; Van Wagener and Rochelle, 2011a; Mathias and Gilmartin, 2014, 2020) are applied to evaluate and compare different carbon

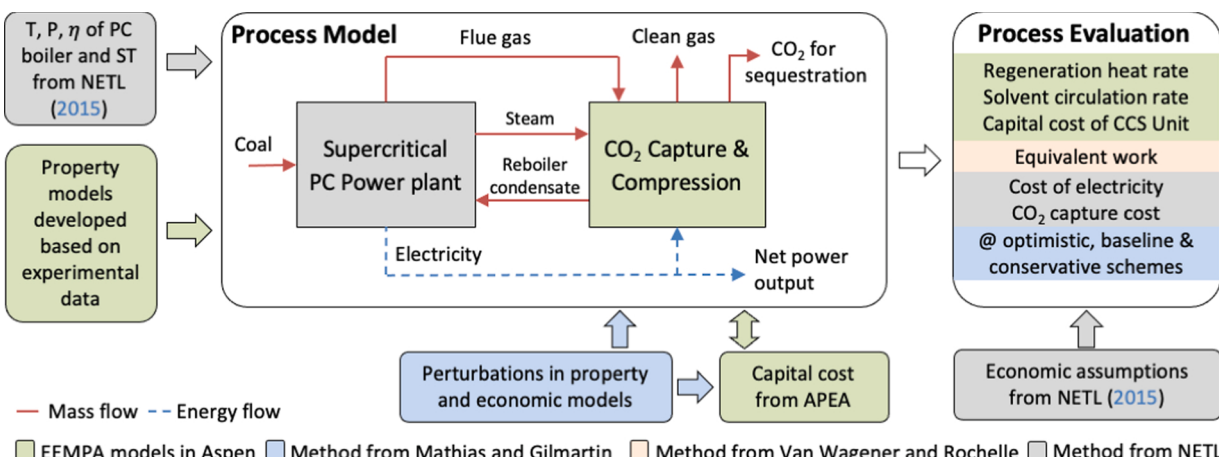


Fig. 3. Analysis approach for techno-economic comparison.

capture technologies, reducing discrepancies related to methods and assumptions. Aspen Process Economic Analyzer (APEA) V10 is used for primary capital cost projection of the carbon capture and compression (CCC) section in the PC power plant. Fig. 3 summarizes the overall analysis approach. The approach for process modeling is detailed in Sections 2.1 to 2.3. The approach for performance and economic evaluations are detailed in Sections 2.4 and 2.5.

2.1. Process modeling and plant configurations

In this study, Case B12B in NETL's cost and performance report (NETL, 2015), a 550 MW supercritical PC power plant with carbon capture using Cansolv solvent, is selected as the baseline for techno-economic comparison. To fully adopt the TEA approach suggested by NETL (2015), process models were developed for the entire

power plant with CCC in Aspen Plus V10. As shown in Fig. 3, coal is fed to the boiler to generate high pressure steam, which is used for power generation in the steam turbine (ST). Low pressure steam is extracted from the ST intermediate stage to supply heat for solvent regeneration in the CCC section. The condensed water from the CCC section is circled back to the boiler as part of the boiler feed water. The flue gas from the PC boiler is sent to the CCC section to produce clean flue gas and high-pressure CO₂ (at 152.7 bar) ready for sequestration. The electricity consumed in the CCC and other sections in the power plant is supplied by the ST as auxiliary load. The net power output is the difference between the ST power generation and the total auxiliary load. In the process model, the operating temperature (T), pressure (P) and efficiency (η) of key unit operations in the supercritical PC power plant (i.e. coal-fired boiler, air blower, steam turbine, cooling tower) are set the same as NETL Case B12B (NETL, 2015). The feed coal flowrate is adjusted to

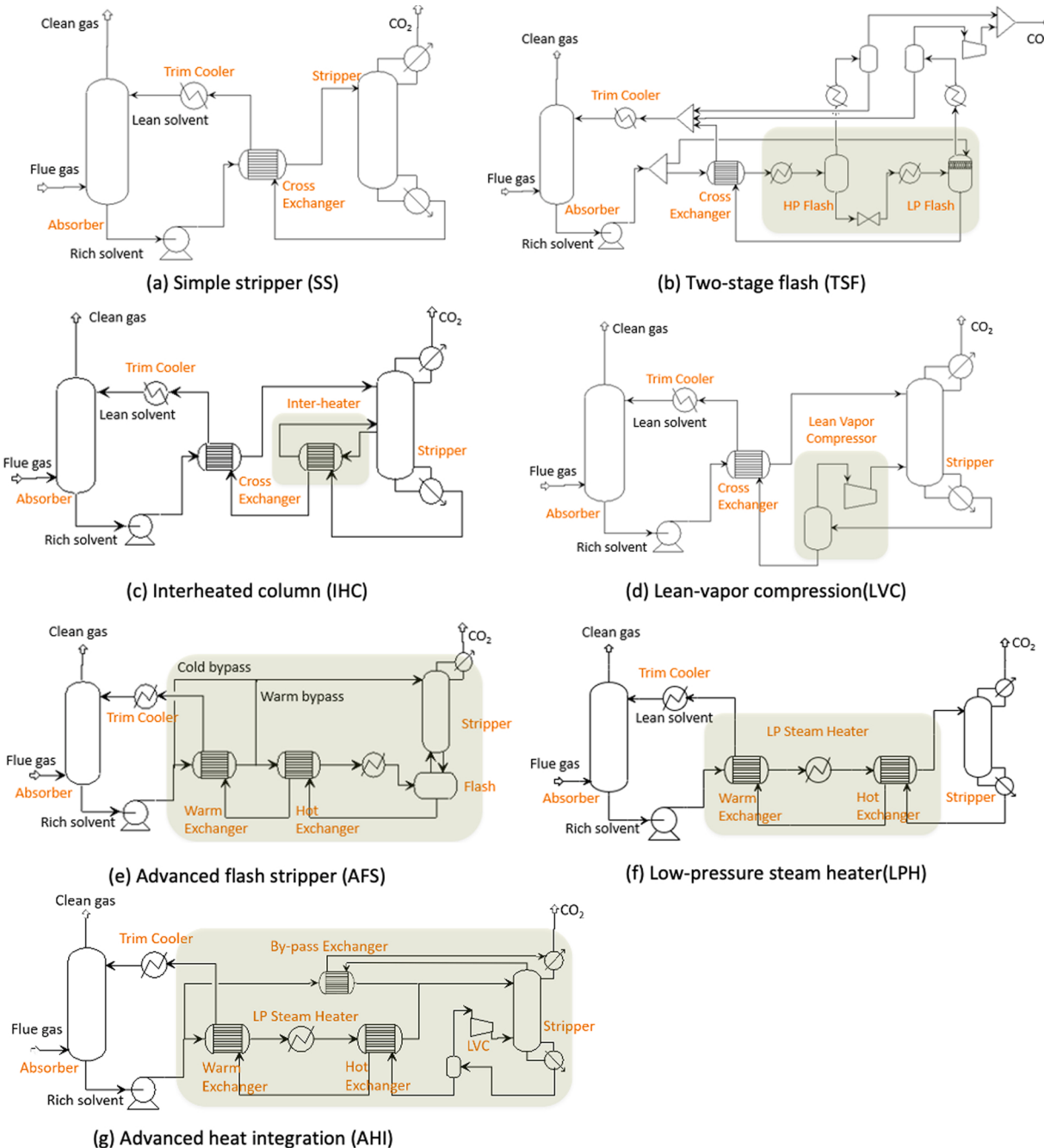


Fig. 4. Configurations for solvent regeneration.

Table 1
Specifications of columns in the carbon capture unit.

	Absorber	Stripper
Calculation type	Rate-based	Rate-based
Number of stages	10	10
Intercooling locations	5, 8	None
Packing type ^a	Mellapak Sulzer 250Y	CMR Koch Metal No.2
Chemistry	Equations (1) and (2)	Equations (1) and (2)
Reactions	Equations (5a) and (5b)	None

^a The packing type is selected based on industrial experience for carbon capture.

achieve a net plant power output of 550 MW.

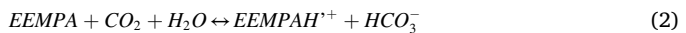
In the CCC section, the flue gas, consisting of 12.9 mol% CO₂, 14.5 mol% H₂O, 68.5 mol% N₂, 3.3 mol% O₂ and 0.8 mol% Ar, is first sent to a three-stage direct contact cooler (DCC) and a flue gas blower before entering the CO₂ absorber. The DCC is comprised with three packed sections, one for trim SO₂ removal, one for flue gas cooling with cooling water (CW) supplied at 15.6 °C (NETL, 2015), and the other for flue gas cooling with chilling water supplied by NH₃ refrigeration cycle. The flue gas inlet temperature to the absorber is set to 15.6 °C based on our previous experience with CO₂BOL solvents for better water management in the solvent circulation system (Mathias et al., 2013; Zheng et al., 2020). Note that in a water lean solvent system moisture in the flue gas may accumulate into the solvent, and therefore may impact the heat rate, absorption kinetics, and physical properties. As a result, additional dehumidification of the incoming flue gas is recommended to reduce the water accumulation in the solvent. The chilled flue gas is then sent to the absorber with two intercoolers, where 90% of CO₂ is removed from flue gas by the lean solvent. The rich solvent from the absorber is then sent to the solvent regeneration system to separate the rich solvent to the CO₂ product and lean solvent. The CO₂ stream is compressed to 152.7 bar for sequestration.

In this study, seven different configurations for solvent regeneration are analyzed, as illustrated in Fig. 4, and the unique pieces of equipment are highlighted in green boxes. Here, SS is the simplest configuration for carbon capture. TSF, LVC, IHC and AFS have been selected as economic favorable configurations for aqueous amine systems by different researchers, of which detailed descriptions can be found in open literature (Van Wagener and Rochelle, 2011a; Scherffius et al., 2013; Walters et al., 2013). LPH and AHI are two new configurations identified as promising because for EEMPA the difference in extrinsic heat capacity ($\dot{m}C_p$) between lean and rich solvents in water-lean solvent systems is much larger than that of aqueous solvent system. This large difference in $\dot{m}C_p$ enables the utilization of a small amount of low-quality steam (at a temperature much lower than reboiler temperature) to preheat rich solvent before it enters the stripper in the LPH configuration. The AHI configuration utilizes a part of the condenser heat and combines the potential benefits from both LVC and LPH.

For all configurations, absorbers and strippers are modeled as rate-based columns, of which more details can be found in Table 1. The

2.2. Property models for EEMPA-H₂O-CO₂ system

In this study, ENRTL-RK is used as the base property method to describe the EEMPA-H₂O-CO₂ system in Aspen Plus, including electrolyte thermodynamics and solution chemistry, reaction kinetics, and transport property modeling. The chemical absorption of CO₂ is represented by Eq.s (1) and (2).



Experimental data are used to regress parameters in the property models. Table 2 summarizes the property parameters selected for regression. The vapor-liquid equilibrium (VLE) data collected from a PTx cell (Mathias et al., 2013; Zhang et al., 2020) at 40 °C, 60 °C, and 75 °C with water concentrations of 0 wt%, 2.4 wt%, and 9 wt%, as shown in Fig. 5, are used to regress the parameters for binary interaction, electrolyte pairs in the ENRTL-RK model and the two chemical-equilibrium equations, given in Eq. (3). Similarly, density and viscosity data measured experimentally at different temperature and CO₂ loading are used to regress model parameters, as shown in Fig. 6. Instead of built-in viscosity model in Aspen Plus, a user model, as shown in Equation (4) (Mathias et al., 2015), is used in the model to provide a better model fitting. Kinetic data measured from wetted-wall column (WWC), as shown in Fig. 7, are used to regress the parameters in the user-defined reaction kinetic models, given in Equation (5) via Aspen Plus built-in Data-Fit Tool. In Aspen Plus, WWC was modeled as a rate-based Rad-Frac column with the same height, operating condition, and form of reaction kinetics specified by Equation (5), where the simulated overall mass transfer coefficient (K_G) was calculated from the stream results and column geometry. In Fig. 7, a negative temperature dependence was observed for K_G experimentally. This unique phenomenon was also observed, validated and discussed in detail for different water-lean carbon capture solvents developed by PNNL (Mathias et al., 2015) and GE Global Research (Whyatt et al., 2017), respectively. The simplified Gibbs-Helmholtz Equation, given in Eq. (6) (Mathias and Connell, 2012; Mathias, 2016), was used to derive the heat of solution from VLE data to ensure thermodynamic consistency. In Eq.s (3) to (6), $K_{eq,i}$, μ , w , T , α_{CO_2} , R_i , C_{Tot} , a , R , ΔH_s , σ and P_{CO_2} represent chemical equilibrium constant, viscosity, weight fraction (CO₂ free), temperature, CO₂ loading, reaction rate, solution molarity, activities, gas constant, heat of solution, bubble point and CO₂ partial pressure, respectively, while A_i , B_i , β , γ , k_{i0} , E_i are the model parameters. In all figures, the experimental data and modeling results are represented by dots and lines, respectively. As observed in Figs. 5–7, the current property package can adequately represent the EEMPA-H₂O-CO₂ system for primary TEA. The model accuracy will be further improved with on-going property measurements and system performance measurements from the laboratory- and bench-scale continuous flow systems (Zhang et al., 2020).

$$K_{eq,i} = A_i + B_i/T \quad (3)$$

$$\ln(\mu) = (w_{EEMPA} \ln(\mu_{EEMPA}) + (1 - w_{EEMPA}) \ln(\mu_{H_2O}) + \gamma w_{EEMPA} (1 - w_{EEMPA})) e^{\alpha_{CO_2} \beta} \quad (4a)$$

columns are sized to have a flooding factor close to but less than 80%. The minimum temperature approach in the cross exchangers is set to 5 °C. The solvent circulation rate is adjusted to achieve 90% CO₂ capture. Lean loading and regeneration pressure are determined by sensitivity studies for low CO₂ capture costs.

$$\ln(\mu_{EEMPA}) = A_1 + A_2/T + A_3 \ln(T) \quad (4b)$$

Table 2
Parameters selected for regressing property models.

Experimental data	Parameter sets	Component i	Component j	Parameters ^a
	Pure component			
VLE	CPDIEC	EEMPA		A
VLE	PLXANT	EEMPA		C_1, C_2
VLE	DHAQRM, DGAQFM	$EEMPAH^+$	$EEMPACO_2^-$	Scalar
VLE	CPAQ	$EEMPAH^+$		C_1
Density	RKTZRA	EEMPA		Scalar
Viscosity	Equation (4b)	EEMPA		A_1, A_2, A_3
	Binary interaction			
VLE	NRTL	H ₂ O	EEMPA	B_{ij}
VLE	NRTL	CO ₂	EEMPA	A_{ij}
VLE	HENRY	CO ₂	EEMPA	A_{ij}, B_{ij}
Density	VLCLK	$EEMPAH^+$	$EEMPACO_2^-$	V_{ca}
Density	VLCLK	$EEMPAH^+$	HCO ₃ ⁻	V_{ca}
Viscosity	Equation (4a)	EEMPA	H ₂ O, CO ₂	β, γ
	Electrolyte Pair			
VLE	GMENCC	EEMPA	$EEMPAH^+, EEMPACO_2^-$	$C_{ca,B}, C_{B,ca}$
VLE	GMENCC	H ₂ O	$EEMPAH^+, EEMPACO_2^-$	$C_{ca,B}, C_{B,ca}$
	Reactions			
VLE	Chemistry	Equation (3)		A_i, B_i
WWC	Reaction kinetics	Equations (5)		k_{i0}, E_i

^a For parameters in Aspen built-in property routes, their definition can be found in the User Guide.

$$R_1 = k_{10} \exp \left[-\frac{E_1}{R} \left(\frac{1}{T} - \frac{1}{313.15} \right) \right] C_{Tot}^2 a_{CO_2} a_{EEMPA} \left(1 - \frac{a_{EEMPAH^+} a_{EEMPACO_2^-}}{a_{CO_2} a_{EEMPA} K_{eq,1}} \right) \quad (5a)$$

$$R_2 = k_{20} \exp \left[-\frac{E_2}{R} \left(\frac{1}{T} - \frac{1}{313.15} \right) \right] C_{Tot}^2 a_{CO_2} a_{EEMPA} a_{H_2O} \left(1 - \frac{a_{EEMPAH^+} a_{HCO_3^-}}{K_{eq,2}} \right) \quad (5b)$$

$$\Delta H_s = -R \left(\frac{\partial \ln P}{\partial (1/T)} \right)_{\sigma(a_{CO_2})} = -R \frac{\ln(P_{CO_2,2}/P_{CO_2,1})}{(1/T_2 - 1/T_1)} \quad (6)$$

2.3. Capital cost estimation of the carbon capture and compression section

In this work, Aspen Process Economic Analyzer (APEA) V10 (with 2016 pricing basis) was used for a primary equipment cost estimation of the carbon capture and compression sections, designed with a single-train configuration for the carbon capture section and a two-train configuration for the CO₂ compression section. Stream information (i.e. T, P, \dot{m}) as well as equipment type specified in the Aspen Plus models are directly ‘exported’ to APEA. Except columns (sized in Aspen Plus) and heat exchangers (sized in Aspen Exchanger Design and Rating (EDR)), all equipment is sized using ASTM standards or other correlations available in APEA (Jiang and Bhattacharyya, 2016, 2017). The materials of construction (MOC) for all project components, were selected based on the operating temperature, composition of the service stream. Except in the absorber, the final selection of MOC was aligned with common industrial practice (Kohl and Nielsen, 1997) and similar to our previous publication (Jiang and Bhattacharyya, 2016, 2017) for aqueous amine-based carbon capture system. For the absorber in EEMPA system, plastic packing (polypropylene in this TEA) was used to replace stainless steel, which was frequently used in aqueous amine system. This inspiration of using plastic is due the superior wetting

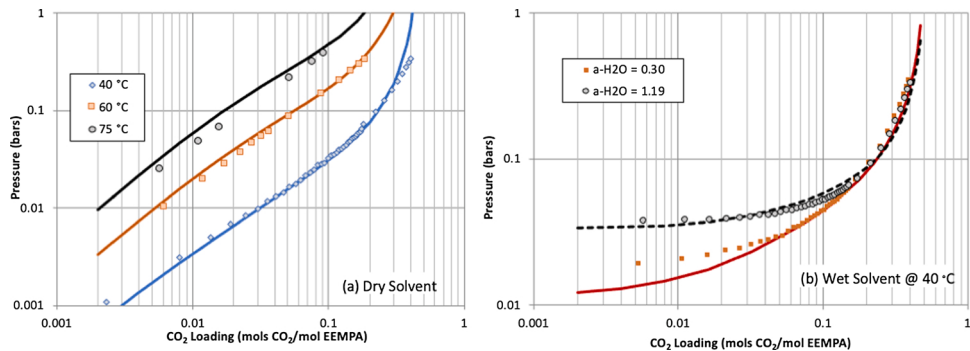


Fig. 5. Vapor-liquid equilibrium of the EEMPA-H₂O–CO₂ system.

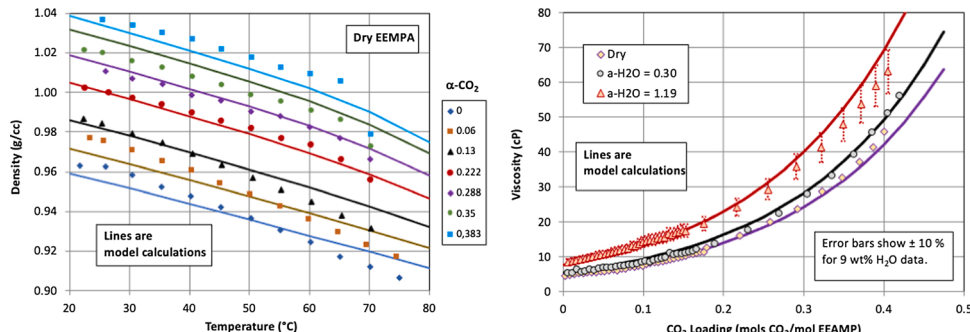


Fig. 6. Density and viscosity of the EEMPA-H₂O–CO₂ system.

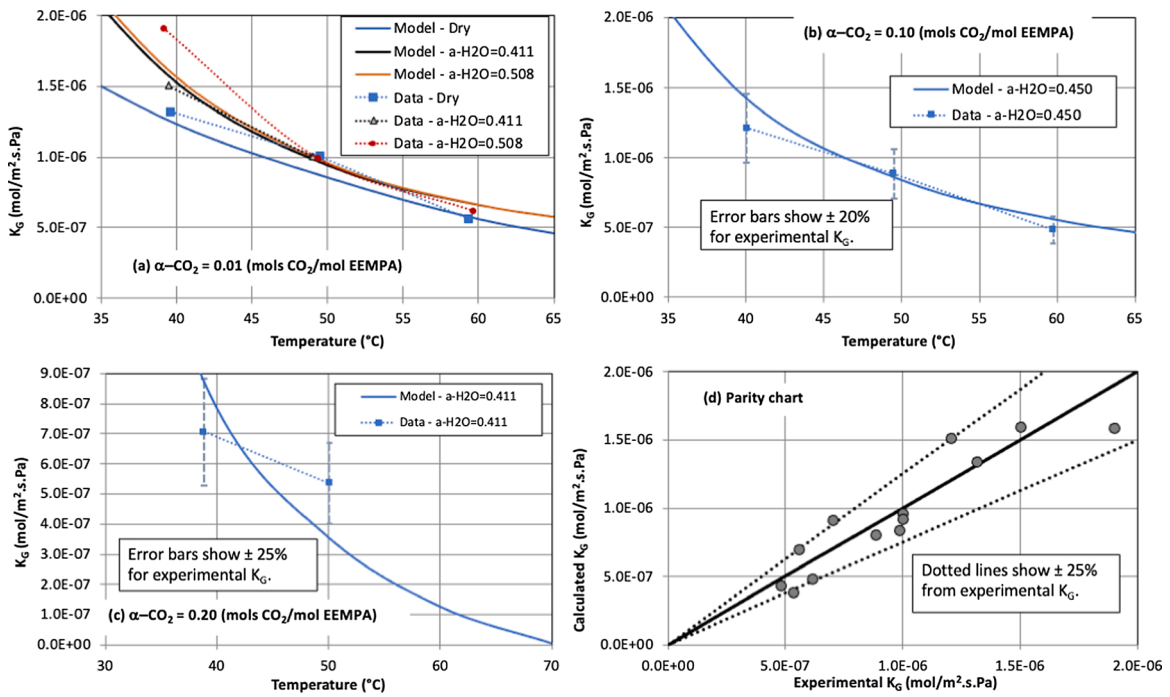


Fig. 7. Kinetic data from wetted-wall column for the EEMPA-H₂O-CO₂ system.

capability of water-lean solvents on plastic (Leclaire and Heldebrant, 2018) and its low cost. Different plastic packings were also tested in our laboratory-scale continuous flow system (Zheng et al., 2020). For all pumps, spares are considered. The equipment cost is then estimated by APEA's built-in Icarus database. A multiplication factor of 2.91, as reported in NETL CaseB12B (NETL, 2015), is applied to the total equipment cost estimated by APEA, to include other costs (from material, labor, Engineer/Procure/Construct contract services, process and project contingencies) and thus estimate the total plant capital cost. Chemical Engineering Plant Cost Index (CEPCI) is used to convert the capital cost projected in the 2016 pricing basis by APEA to the 2011 pricing basis used in NETL CaseB12B (NETL, 2015), and thus enable a fair comparison. Table 3 provided detailed equipment list, along with sizes and bare equipment cost projections from APEA of key equipment in the EEMPA-based SS configuration with a lean loading of 0.045 mol CO₂/mol solvent and a regeneration pressure of 1.81 bar.

2.4. Approach for performance and cost projections

As shown in Fig. 3, the approach proposed by NETL (2015) was used to calculate the cost of electricity (COE) and the carbon capture cost. Particularly, Aspen Plus models were used to estimate the net power output (W_{net}), CO₂ emission, plant efficiency (η_{HHV} , defined in Eq. (7)), and the capital cost of the CCC section. The price of EEMPA is assumed to be \$10/kg for calculating variable cost, since it can be synthesized from inexpensive raw materials by a single-step approach (Zhang et al., 2020). Note that the carbon capture cost is insensitive to the price of solvent as long as it is at the same order of magnitude as aqueous amines due to the relatively small solvent loss (NETL, 2010, 2015). The fixed operating cost, variable cost and capital cost of non-carbon capture sections in the power plant are calculated from the values reported in NETL Case B12B (NETL, 2015) and scaled proportional to throughputs on a USD per kWe net power generation basis. The cost of electricity (COE) was calculated by adding up fuel cost, capital cost (annualized), variable cost and fixed operating cost. The carbon capture cost is calculated by Eq. (8), where COE does not include the CO₂ transportation and storage (T&S) cost.

$$\eta_{HHV} = W_{net}/(\dot{m}_{Coal} \times HHV_{Coal}) \quad (7)$$

$$Cost_{CO_2captured} = (COE_{CCS} - COE_{NonCCS})/CO_2Captured \quad (8)$$

The equivalent work approach, proposed by Van Wagener and Rochelle (2011a), is also applied in this work for process evaluation, which allows a quick comparison of various energy penalties of carbon capture between different solvents and configurations without modeling the entire power plant. As defined in Eq. (9), the total equivalent work of carbon capture (W_{Total}) in $kJ_e/molCO_2$ can be calculated by adding up the energy consumption from reboiler or heaters (W_h), cooling (W_{cl}), refrigeration (W_f), pumping (W_p), and compression (W_{cp}). Here, W_h is evaluated from the Carnot efficiency and solvent regeneration heat rate by Eq. (10), while others can be found directly from the carbon capture and compression (CCC) section in Aspen Plus models. In Eq. (10), T_r , T_{sink} , and Q_r are the regeneration temperature, heat sink temperature (40 °C in this work), and regeneration heat rate per mole captured CO₂, respectively.

$$W_{Total} = W_h + W_{cl} + W_f + W_p + W_{cp} \quad (9)$$

$$W_h = 0.9 \left(\frac{T_r + 5 - T_{sink}}{T_r + 5} \right) Q_r \quad (10)$$

2.5. Perturbation scheme analysis

As mentioned, uncertainties in property model and capital cost estimation may impact the projections of process performance and carbon capture costs. In this work, a simple perturbation scheme analysis (Mathias and Gilmartin, 2014, 2020) was conducted to provide an optimistic and conservative boundary of the process performance and cost projections when comparing different process configurations. Note that the perturbation scheme analysis focuses on the impacts of uncertainties from physical quantities on process simulation and economic analysis rather than the uncertainties from abstract model parameters. Therefore, perturbations are only applied to a limited number of parameters, rather than all parameters. Parameters were chosen to apply reasonable perturbations in the simulated property quantities, that is,

Table 3Equipment list in APEA for equipment cost projection^a.

Equipment	Spares	Size	Equipment Cost (MM\$, 2016)	Reference
Blower/Compressors				
Flue gas blower		5.54 MW	9.26	Aspen Icarus
CO ₂ compressor		38.48 MW	45.98	NETL, 2015
Lean vapor compressor ^b				Aspen Icarus
Heat Exchangers				
DCC coolers (shell & tube)		549 GJ/hr	5.05	Aspen Icarus
Absorber intercoolers (plate & frame)		615 GJ/hr	4.62	Aspen Icarus
Cross exchanger (plate & frame)		1642 GJ/hr	13.65	Aspen Icarus
Trim cooler (plate & frame)		410 GJ/hr	3.82	Aspen Icarus
Stripper reboiler (shell & tube)		1046 GJ/hr	11.74	Aspen Icarus
Stripper condenser (shell & tube)		30 GJ/hr	0.07	Aspen Icarus
HP/LP flash pre-heaters (shell & tube) ^b				Aspen Icarus
Columns/Vessels				
DCC column		17 m (D), 12 m (H)	16.76	Aspen Icarus
Absorber		20 m (D) ^c , 21 m (H)	24.43 ^d	Aspen Icarus
Stripper		10 m (D), 12 m (H)	8.95	Aspen Icarus
Absorber overheat accumulator			0.36	Aspen Icarus
Reboiler condensate drum			0.07	Aspen Icarus
HP/LP flash condensate drums ^b				Aspen Icarus
HP/LP flash vessels ^b				Aspen Icarus
Lean vapor compressor drum ^b				Aspen Icarus
Pumps				
DCC water circulation pumps	Yes	1.42 MW	2.74	Aspen Icarus
Absorber wash section pump	Yes		0.09	Aspen Icarus
Rich solvent pump	Yes	1.49 MW	2.69	Aspen Icarus
Lean solvent pump	Yes	1.41 MW	2.16	Aspen Icarus
Stripper reflux pump	Yes		0.01	Aspen Icarus
Others				
Solvent storage tank		30 days storage	1.98	Aspen Icarus
Refrigeration plant		78 GJ/hr	5.47	Aspen Icarus
Miscellaneous ^e			7.90	

^a HP = high pressure, LP = low pressure, DCC = direct contract cooler, D = diameter, H = (packing) height.^b Only used in the LVC or TSF configuration.^c The absorber diameter can be as large as 20 m for a commercial-scale CO₂ capture plant (Scherffius et al., 2013).^d May increase to 46.8 MM\$, if stainless steel packing is used in the absorber.^e 4.5% of total equipment cost.

about 10% changes in VLE, kinetics, and viscosity. Those disturbances consequently lead to changes in process design, and estimations of mass and energy balances. For VLE, as shown in Fig. 5, the simulated curves can be impacted by equilibrium constants of chemical reactions (K_{eq}), Henry's constant for physical solubility, and binary/pair interaction parameters, when using ENRTL-RK thermal package in Aspen Plus. Here, the binary parameter K_{eq}/A_1 (in Eq. (3)), with the strongest impact among all above candidates, was selected to perturbate the VLE curves. For absorption kinetics, as shown in Fig. 7, the simulated K_G curve can be impacted by reaction kinetic parameters in Equation (5), mass-transfer coefficients and interfacial area of the contacting device, etc. In this work, the liquid mass transfer coefficient factor in the absorber was selected to perturb the K_G curves. The $\pm 10\%$ perturbation in viscosity was only considered when designing heat exchangers in Aspen EDR, since it is proven to be of lesser importance for simulating and designing other equipment in a solvent-based carbon capture unit (Mathias and Gilmartin, 2020). In addition, a perturbation of $+30\%/-20\%$ was applied to the capital cost projection as recommended by the Association for the Advancement of Cost Engineering (AACE) for Class 5 estimation. All perturbations leading to lower carbon capture cost projection are grouped and applied when analyzing the optimistic scheme, while all perturbations leading to higher cost projection are applied when analyzing the conservative scheme. Since it is not as mathematically intensive as other rigorous uncertainty quantification approaches, this approach can quickly provide design engineers "a feel of the process".

3. Results and discussions

With the approach described in Section 2, primary techno-economic

analyses are performed to evaluate EEMPA for post-combustion carbon capture and to compare different configurations. Particularly, Section 3.1 presents sensitivity studies to evaluate the impacts and the optimal values of key process design variables (i.e. lean loading and regeneration pressure). Section 3.2 provides a detailed perturbation analysis for the SS configuration. Section 3.3 compares the key performance and economic projections of seven process configuration at the baseline, optimistic and conservative schemes.

3.1. Impacts of lean loading and regeneration pressure

The selection of CO₂ loading in the lean solvent and the pressure for solvent regeneration may significantly impact the performance and economic projections of a water-lean solvent system. Sensitivity studies were performed to determine the optimal lean loading and regeneration pressure for EEMPA system with the lowest CO₂ capture cost. The detailed impact analysis for the SS (Fig. 4(a)) and TSF (Fig. 4(b)) configurations are provided in Figs. 8–10. For the IHC, LVC, AFS, LPH, and AHI configurations, the impacts of lean loading and regeneration pressure are almost identical to the SS configuration. Similarly, Van Wagenen and Rochelle (2011a) reported a less than 5% difference in the optimal lean loading between different configurations for aqueous amine system.

For the SS configuration, Fig. 8 (f) suggests an optimal lean loading of 0.1125 mol CO₂/mol solvent with the lowest carbon capture cost of \$49.4/tonne CO₂ at a regeneration pressure of 1.81 bar. As observed from Fig. 8(b), the reboiler temperature of the EEMPA system reduces from 119 °C to 85 °C as the lean loading increases from 0.045 mol CO₂/mol solvent to 0.135 mol CO₂/mol solvent. A lower energy penalty is expected at lower solvent regeneration temperatures, because of the less

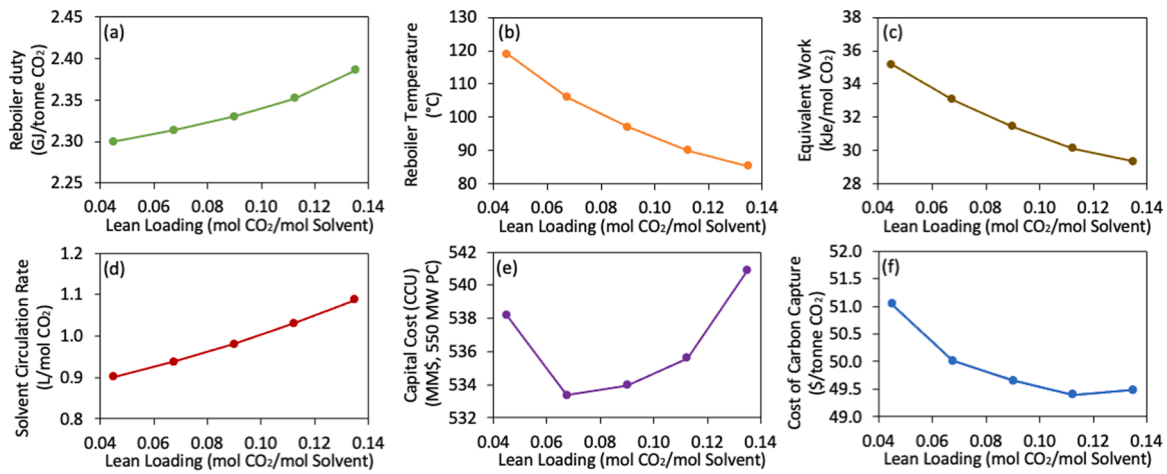


Fig. 8. Impact of lean loading on the simple stripper configuration (regeneration pressure = 1.81 bar).

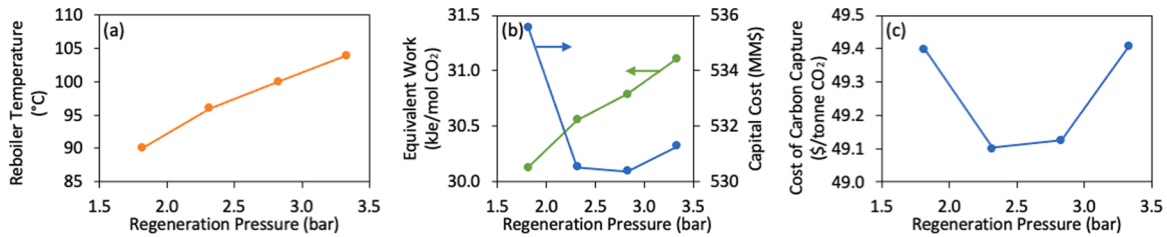


Fig. 9. Impact of regeneration pressure on the simple stripper configuration (lean loading = 0.1125 mol CO₂/mol solvent).

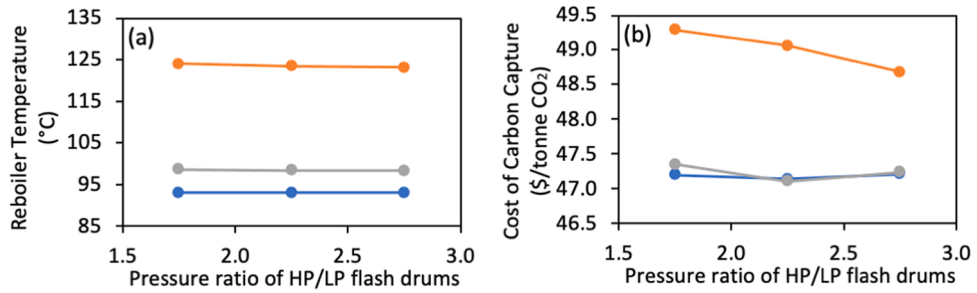


Fig. 10. Impact of design variables on the two-stage flash configuration.

reduction on ST power regeneration in the PC power plant. Consequently, Fig. 8(c) indicates that the total equivalent work of carbon capture decreases monotonically with the increasing lean loading. However, for a fixed CO₂ capture rate, 90% in this work, the solvent circulation rate, as shown in Fig. 8(d) increases with the increasing lean loading, as the solvent working capacity (defined as the difference between rich and lean loadings) decreases. Consequently, the reboiler duty, especially the sensible heat, increases, as shown in Fig. 8(a), while larger columns and solvent circulation pumps are required during the design. The impact of lean loading on the capital cost is complicated, as shown in Fig. 8(e). In a carbon capture unit, the three major capital items are absorber, stripper and cross exchanger. A higher lean loading will lead to larger column sizes, but a lower design temperature for stripper and exchanger, which have opposite impacts on the capital cost. For the cross exchanger, with a fixed approach temperature, its size is dominated by the heat duty ($\dot{m}C_p\Delta T$), when phase change is negligible. The flow rate (\dot{m}) increases with lean loading, while the temperature change (ΔT) decreases because of the lower regeneration temperature. Taking all of the above impacts into consideration, Fig. 8(f) indicates that the carbon capture cost will first decrease and then increase with

the increasing lean loading.

Fig. 9 shows the impact of regeneration pressure on the primary performance parameters for a SS configuration. Here, an optimal regeneration pressure of 2.32 bar was identified for the SS configuration, with a carbon capture cost of \$49.1/tonne CO₂. With an increasing regeneration pressure, the regeneration temperature increases as shown in Fig. 9(a) leading to a higher equivalent work, as shown in Fig. 9(b), while the electricity consumption and capital cost of CO₂ compressor can be significantly reduced. Consequently, the carbon capture cost predictions in Fig. 9 decrease at the beginning and then increases as the regeneration pressure increases from 1.81 bar to 3.33 bar. The impacts of lean loading and regeneration pressure on the TSF configuration are similar to the SS configuration and illustrated in Fig. 10, where LL and LP represent the lean loading in mol CO₂/ mol solvent, and the pressure of LP flash drum, respectively. The results suggest the lowest carbon capture cost of \$47.1/tonne CO₂ for the TSF configuration can achieved at a lean loading of 0.1125 mol CO₂/mol solvent and a pressure ratio of 2.25.

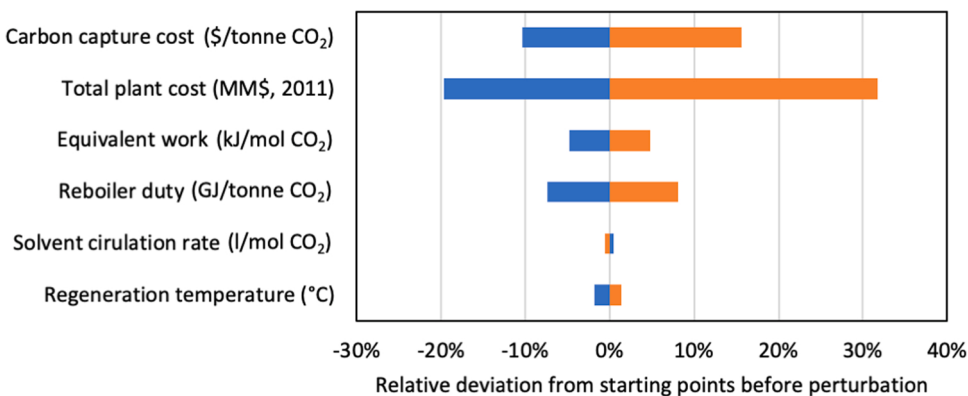


Fig. 11. Projected impact on key process and economic predictions as a result of the perturbation approach outlined in Section 2.5. Note the fixed parameters were the configuration (simple stripper), lean loading (0.1125 mol CO₂/mol solvent), and regeneration pressure (2.32 bar).

3.2. Impacts of uncertainties in property and cost models

Next, a high-level perturbation scheme analysis is conducted to provide optimistic and conservative boundaries for the key performance and economic measures of the EEMPA system and to quantify the potential impacts of uncertainties in property and cost models (approach detailed in Sections 2.2 and 2.5). The results for the perturbation analysis for the SS configuration are shown in Fig. 11. Here, a +/− 10% perturbation in key property measures and a +30%/-20% perturbation in capital cost projection show a ±5% deviation in the estimation of equivalent work consumption, a +8%/-7% deviation in the estimation of reboiler duty, a less than 3% deviation in the estimation of solvent circulation rate and regeneration temperature, and a +16%/-10% deviation in the estimation of carbon capture cost.

Note that, for the SS configuration, uncertainties in the capital cost

estimation contributes to about 80% (about \$5.2/tonne CO₂) of the total deviations in the estimation of carbon capture cost, while the remaining 20% comes from the uncertainties in property models (about \$1.3/tonne CO₂). As discussed in Section 3.1, the largest difference in carbon capture cost for SS is about \$2.0/tonne CO₂ between different operation conditions, which is at the same order of magnitude of the potential deviation in cost estimation. Therefore, it can be concluded that the current model does provide reasonable trends when analyzing the impact of lean loading and regeneration pressure, while the optimal values may be subject to small changes as the property model is refined with on-going experimental data collection.

3.3. Primary comparisons of different configurations

Similar analyses to those discussed in Sections 3.1 and 3.2 were

Table 4
Results summary for 90% CO₂ capture in a 550 MW PC power plant with all configurations.

Solvent	MEA ^a	Cansolv ^b	EEMPA	TSF	LVC	IHC	LPH	AFS	AHI
Configuration	SS	LVC	SS	TSF	LVC	IHC	LPH	AFS	AHI
Operating conditions									
Lean loading (mol CO ₂ /mol solvent)	0.275		0.113	0.113	0.113	0.113	0.113	0.113	0.113
Rich loading (mol CO ₂ /mol solvent)	0.488		0.328	0.328	0.328	0.328	0.328	0.328	0.328
Water content (wt%)	70		1.6	1.6	1.6	1.6	1.6	1.6	1.6
Regeneration temperature (°C)	116.0		96.0	98.4	87.5	95.7	95.7	105.0	87.5
Regeneration pressure (bar)	1.62	1.98	2.32	5.2/2.3	2.32	2.32	2.32	2.32	2.32
Performance measures									
Reboiler heat rate (GJ/tonne CO ₂)	3.55	2.48	2.35	2.36	2.33	2.34	2.32	2.34	2.30
Solvent circulation rate (l/mol CO ₂)	0.99		1.03	1.04	1.03	1.03	1.03	1.03	1.03
Coal feed (tonne/hr) ^c		224.8	212.7	211.4	211.7	212.7	211.4	214.4	210.8
CO ₂ emission (kg/kWe-hr)		0.097	0.091	0.090	0.090	0.091	0.090	0.092	0.090
Net plant efficiency (%), HHV)		32.50	34.30	34.50	34.46	34.31	34.51	34.04	34.61
Equivalent work ^d (kJ _e /mol CO ₂)									
Heating	36.8	25.7	15.2	15.7	13.2	15.1	13.8	16.9	12.3
Cooling		2.4	1.1	2.5	2.5	2.5	2.5	2.5	2.5
Refrigeration				0.7	0.7	0.7	0.7	0.7	0.7
Reclaimer ^e			0.1	0.1	0.1	0.1	0.1	0.1	0.1
Pumping		0.09	0.17	0.21	0.67	0.21	0.21	0.21	0.21
Compression (including LVC)		13.2	14.4	11.9	10.0	12.3	11.9	11.9	12.3
Total	52.6	39.5	30.6	29.7	29.0	30.4	29.2	32.3	28.1
Economic measures (2011 pricing basis)									
Cost of electricity (€/kWe-hr)		14.27	13.14	12.95	13.09	13.12	13.08	13.24	13.03
Total plant cost of CCS (MM\$) ^c		632.0	530.5	496.8	531.2	525.4	531.5	533.0	527.9
Carbon capture cost		58.3	49.1	47.1	48.8	48.9	48.7	49.8	48.3

^a For aqueous MEA, performance measures and equivalent work are evaluated based on the historical NETL Case 12 (NETL, 2010). Economic measures of MEA are not reported due to significant differences in economic assumptions and baseline PC plant efficiency between the historical and recent NETL reports (NETL, 2010, 2015).

^b NETL Case B12B (NETL, 2015).

^c The PC power plant with CCS is scaled to a net power output of 550 MW. Therefore, the flue gas flowrate and CO₂ emission are lower at a higher net power efficiency.

^d The definition and calculation methods of equivalent work were detailed in Section 2.4.

^e For all EEMPA cases, the energy required in solvent reclaimer is assumed to be the same as Cansolv (NETL, 2015).

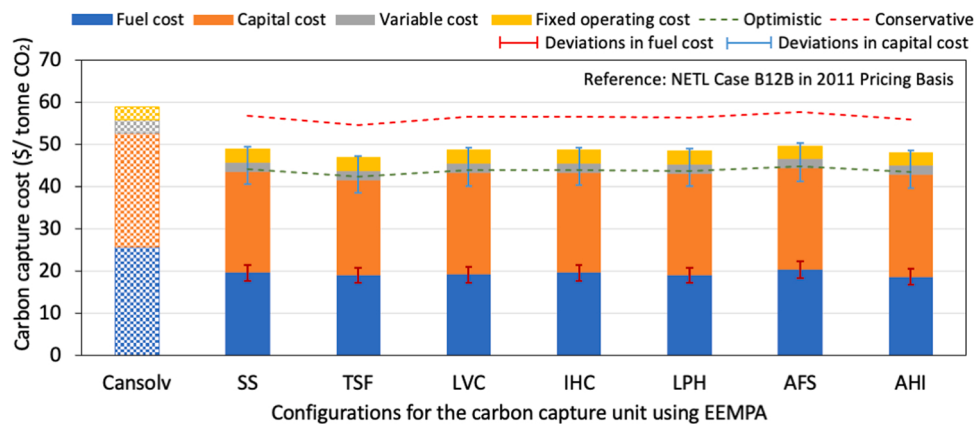


Fig. 12. Breakdown in carbon capture costs of various process configurations with EEMPA.

conducted for the other process configurations. Table 4 summarizes key performance and economic measures at the baseline scheme for EEMPA and the comparison with NETL's baseline cases with MEA (NETL, 2010) and Cansolv (NETL, 2015). Additionally, Fig. 12 provides a detailed cost breakdown. Here, the solid bars present the cost at the baseline scheme; the dashed lines and error bars represent the deviations in cost estimations at the optimistic and conservative schemes.

As shown in Table 4, all EEMPA cases have much lower energy penalty than MEA and Cansolv, due to the “water-lean” attribute of EEMPA. The pumping work of EEMPA is higher because of the slightly higher viscosity. The EEMPA cases also required additional energy and capital investment for flue gas chilling via NH₃ refrigeration cycle for better performance, which is not required by MEA and Cansolv. However, the magnitude of refrigeration was only 2% of the total energy consumption, and 3–4% of total capital investment, respectively. The energy penalties rank as AFS > SS > IHC > TSF > LPH > LVC > AHI in terms of total equivalent work. It is noted that the relative difference in total equivalent work is about 15% between the best and worst EEMPA cases. As discussed in Section 3.2, a +/− 10% deviation in equivalent work estimation is expected between the optimistic, baseline and conservative schemes. Therefore, the current model is sufficient to predict trends and provide a primary comparison. In addition, because of the low water content of EEMPA, compared to aqueous amine systems, configurations such as LVC and AFS were not predicted to provide significant reductions in energy penalty and carbon capture cost. It is expected since LVC and AFS are originally proposed for aqueous amine solvents because of their abilities to offer better water management (Scherffius et al., 2013; Lin and Rochelle, 2014). Among all configurations, AHI was shown to be the most energy efficient option for EEMPA because it is highly heat integrated (as shown in Fig. 4(g)), providing the lowest reboiler heat rate, lowest equivalent work, and highest net plant efficiency. With the AHI configuration, EEMPA was estimated to provide a reboiler heat rate of 2.3 GJ/tonne CO₂, 35% lower than MEA and 18% lower than Cansolv. The corresponding equivalent work for EEMPA in the AHI configuration was 28.1 kJ_e/mol CO₂, which is 47% lower than MEA and 29% lower than Cansolv. The reduction in equivalent work is much larger than that in reboiler heat rate, because EEMPA can be regenerated at lower temperature and higher pressure. However, AHI is a more complicated process arrangement compared to the other configurations, which may reduce its overall attractiveness. Note that, our previous study (Zheng et al., 2020) indicates that with a lower lean loading (0.045 mol CO₂/mol solvent), a reboiler heat rate of 2.0 GJ/tonne CO₂ can be achieved with EEMPA and the AHI configuration, at the expense of higher reboiler temperature and therefore higher equivalent work and carbon capture cost (\$50.6/tonne CO₂). This new design provides a lower equivalent work and carbon capture cost at the expense of a slightly elevated reboiler duty.

Fig. 12 shows a breakdown of the individual predicted carbon

capture costs for each of the process configurations assessed in the current study. The data in Fig. 12 show carbon capture costs for the EEMPA process arrangements ranging from \$47.1/tonne CO₂ to \$49.8/tonne CO₂. The optimistic and conservative ranges for these costs are also shown in Fig. 12. These ranges were based on the results from the perturbation analysis and were approximately +8/−5 \$/tonne CO₂ higher and lower, respectively, for each process configuration. Note that in all cases shown in Fig. 12 the conservative end of the EEMPA estimates were lower than the Cansolv reference. The dominant contributors to the lower carbon capture costs for EEMPA were the lower energy penalty and the ability to use less expensive plastic packing in the absorber (Leclaire and Heldebrant, 2018; Jiang et al., 2019a, b). Similar to aqueous amine systems, the fuel and capital costs were still the two largest contributors to the total carbon capture cost for EEMPA. Compared with the values in Fig. 1, the capital cost was a larger fraction of the total carbon capture cost for EEMPA compared to aqueous amines because of the significant improvement in energy efficiency. Additionally, the cross heat exchanger in the EEMPA system is larger than that of aqueous amine system due the correspondingly lower thermal conductivity. Note that the fixed and variable costs for EEMPA in Fig. 12 were nearly the same, and similar to that of Cansolv. This similarity is due to the fact that only small changes in plant configurations were made, which does not significantly impact the number of operators and the amount of solvent loss.

Among all process configurations shown in Fig. 12, TSF has the lowest predicted carbon capture cost due to savings in capital costs by replacing the stripper with two flash drums, even though its corresponding regeneration heat rate is slightly higher. AFS has the highest carbon capture cost because it has negligible saving in energy penalty but comes with a considerable increase in plant complexity. In addition to TSF, AHI can also bring a significant reduction in carbon capture cost comparing with SS, about \$0.8/tonne CO₂, due to energy savings, but potentially higher capital costs. Despite these advantages and disadvantages, the difference in carbon capture costs between SS, LVC, IHC, and LPH is less than \$0.4/tonne CO₂, which is not significant enough to necessarily differentiate one process over another at the present level of analysis.

4. Conclusions

In summary, a property package was developed and validated for the EEMPA-H₂O-CO₂ system. Plant-wide process models were developed in Aspen Plus for 90% post-combustion carbon capture from a supercritical coal-fired plant with EEMPA in seven different process configurations. Optimal lean loading and regeneration pressure were identified from sensitivity studies. A primary techno-economic comparison, subject to a +16% / − 10% deviation in the estimation of carbon capture costs, was conducted. The results showed that even with the simplest process

configuration (simple stripper, SS) the energy penalty of EEMPA system is 42% lower than the MEA comparison case, and 23% lower than Cansolv. Energy penalties were predicted to further reduce with advanced solvent regeneration configurations. For EEMPA, AHI provides the lowest energy penalty of 28.1 kJ/mol CO₂, about 8% lower than the standard SS configuration. However, configurations such as LVC and AFS, with significant efficiency gains proven for aqueous amines, did not show significant predicted reductions in energy and cost for EEMPA. Based on the current analysis, TSF is the deemed the best configuration for EEMPA, offering the lowest carbon capture cost of \$47.1/tonne CO₂ due to its lowest capital cost investment. For EEMPA, SS and TSF are also predicted to provide carbon capture costs 16% and 19% lower than Cansolv, respectively. Further reduction in carbon capture cost with water-lean solvents could be possible with further solvent development and process optimization.

CRediT authorship contribution statement

Yuan Jiang: Methodology, Writing - original draft. **Paul M. Mathias:** Methodology, Writing - review & editing. **Charles J. Freeman:** Supervision, Writing - review & editing. **Joseph A. Swisher:** Writing - review & editing. **Richard F. Zheng:** Resources, Writing - review & editing. **Greg A. Whyatt:** Writing - review & editing. **David J. Heldebrant:** Supervision, Project administration, Writing - review & editing.

Declaration of Competing Interest

The authors declare that they have no known competing financial interests or personal relationships that could have appeared to influence the work reported in this paper.

Acknowledgements

The authors would like to acknowledge the US Department of Energy Office of Fossil Energy FWP70924 (managed by NETL) for funding this project and the Pacific Northwest National Laboratory (PNNL) for facilities. The authors would also like to thank Robert Perry for insights into diamine behavior and fruitful discussions. Battelle proudly operates PNNL for DOE under Contract DE-AC05-76RL01830.

References

- Ahn, H., Luberti, M., Liu, Z., Brandani, S., 2013. Process configuration studies of the amine capture process for coal-fired power plants. *Int. J. Greenhouse Gas Control* 16, 29–40.
- Amrollahi, Z., Ertesvag, I.S., Bolland, O., 2011. Optimized process configurations of post-combustion CO₂ capture for natural-gas-fired power plant – exergy analysis. *Int. J. Greenhouse Gas Control* 5 (6), 1393–1405.
- Bui, M., Adjiman, C.S., Bardow, A., Anthony, E.J., Boston, A., Brown, S., Fennell, P.S., Fuss, S., et al., 2018. Carbon capture and storage (CCS): the way forward. *Energy Environ. Sci.* 11, 1062–1176.
- EPA, 2020. Sources of Greenhouse Gas Emissions. United States Environmental Protection Agency [last access on 08/12/2020]. <https://epa.gov>.
- Heldebrant, D.J., Glezakou, V., Koech, P.K., Mathias, P., Cantu, D., Rousseau, R., Malhotra, D., Bhakta, M., Bearden, M.D., Freeman, C.J., Zheng, F., 2014. Evaluating transformational solvent systems for post-combustion CO₂ separations. *Energy Procedia* 63, 8144–8452.
- Heldebrant, D.J., Koech, P.K., Glezakou, V., Rousseau, R., Malhotra, D., Cantu, D.C., 2017. Water-lean solvents for post-combustion CO₂ capture: fundamentals, uncertainties, opportunities, and outlook. *Chem. Rev.* 117 (14), 9594–9654.
- Jiang, Y., Bhattacharyya, D., 2016. Techno-economic analysis of a novel indirect coal-biomass to liquids plant integrated with a combined cycle plant and CO₂ capture and storage. *Ind. Eng. Chem. Res.* 55 (6), 1677–1689.
- Jiang, Y., Bhattacharyya, D., 2017. Techno-economic analysis of direct coal-biomass to liquids (CBTL) plants with shale gas utilization and CO₂ capture and storage (CCS). *Appl. Energy* 189, 433–448.
- Jiang, Y., Jones, S.B., Zhu, Y., Snowden-Swan, L., Schmidt, A.J., Billing, J.M., Anderson, D., 2019a. Techno-economic uncertainty quantification of algal-derived biocropic via hydrothermal liquefaction. *Algal Res.* 39, 101450.
- Jiang, Y., Mathias, P.M., Whyatt, G., Freeman, C.J., Zheng, R., Heldebrant, D.J., 2019b. Techno-economic analysis of post-combustion carbon capture with a 3rd generation water-lean solvent. In: In Proceeding: 2019 AIChE Annual Meeting. Orlando FL, Nov 10-15, 2019.
- Jones, M.N., Frutiger, J., Ince, N.G., Sin, G., 2019. The Monte Carlo driven machine learning enhanced process simulator. *Comput. Chem. Eng.* 125, 324–338.
- Kohl, A., Nielsen, R., 1997. Gas Purification, 5th ed. Gulf Professional Publishing, Houston, TX.
- Lail, M., Tanthana, J., Coleman, L., 2014. Non-aqueous solvent (NAS) CO₂ capture process. *Energy Procedia* 63, 580–594.
- Leclaire, J., Heldebrant, D.J., 2018. A call to (green) arms: a rallying cry for green chemistry and engineering for CO₂ capture, utilization and storage. *Green Chem.* 20 (22), 5058–5081.
- Lin, Y., Rochelle, G.T., 2014. Optimization of advanced flash stripper for CO₂ capture using piperazine. *Energy Procedia* 63, 1504–1513.
- Mathias, P.M., Gilmartin, J.P., 2014. Quantitative evaluation of the effect of uncertainty in property models on the simulated performance of solvent-based CO₂ capture. *Energy Procedia* 63, 1171–1185.
- Mathias, P.M., Gilmartin, J.P., 2020. Effect of uncertainty in property models on the simulation performance of solvent-based CO₂ capture – study of aqueous AMP as solvent. submitted to International Journal of Greenhouse Gas Control.
- Mathias, P.M., Afshar, K., Zheng, F., Bearden, M., Freeman, C.J., Andreia, T., Koech, P.K., Kutnyakov, I., Zwoster, A., Smith, A.R., Jessop, P.G., Ghaffari Nik, O., Heldebrant, D.J., 2013. Improving the regeneration of CO₂-binding organic liquids with a polarity change. *Energy Environ. Sci.* 6, 2233.
- Mathias, P.M., Zheng, F., Heldebrant, D.J., Zwoster, A., Whyatt, G., Freeman, C.M., Bearden, M.D., Koech, P., 2015. Measuring the absorption rate of CO₂ in nonaqueous CO₂-binding organic liquid solvents with a wetted-wall apparatus. *ChemSusChem* 8, 3617–3625.
- Morgan, J., Chinen, S.A., Anderson-Cook, C., Tong, C., Carroll, J., Saha, C., Omell, B., Bhattacharyya, D., Matuszewski, M., Bhat, K.S., Miller, D.C., 2020. Development of a framework for sequential Bayesian design of experiments: application to a pilot-scale solvent-based CO₂ capture process. *Appl. Energy*, 114533.
- NETL, 2010. Cost and Performance Baseline for Fossil Energy Plants, Volume 1: Bituminous Coal and Natural Gas to Electricity, Revision 2, DOE/NETL-2010/1397. November 2010.
- NETL, 2015. Cost and Performance Baseline for Fossil Energy Plants, Volume 1a: Bituminous Coal (PC) and Natural Gas to Electricity, Revision 3, DOE/NETL-2015/1723. July 2015.
- Sakkwattanapong, R., Aroonwilas, A., Veawab, A., 2005. Behavior of reboiler heat duty of CO₂ capture plants using regenerable single and blended alkanolamines. *Ind. Eng. Chem. Res.* 44 (12), 4465–4473.
- Scherffius, J.R., Reddy, S., Klumppyan, J.P., Armpriester, A., 2013. Large-scale CO₂ capture demonstration plant using fluor's econamine FG PlusSM technology at NRG's WA parish electric generating station. *Energy Procedia* 37, 6553–6561.
- Stowe, H.M., Hwang, G.S., 2017. Fundamental understanding of CO₂ capture and regeneration in aqueous amines from first-principles studies: recent progress and remaining challenges. *Ind. Eng. Chem. Res.* 56, 6887–6899.
- Van Wagener, D.H., Rochelle, G.T., 2011a. Stripper configurations for CO₂ capture by aqueous monoethanolamine. *Chem. Eng. Res. Des.* 89, 1639–1646.
- Van Wagener, D.H., Rochelle, G.T., 2011b. Stripper configurations for CO₂ capture by aqueous monoethanolamine and piperazine. *Energy Procedia* 4, 1323–1330.
- Walters, M.S., Dunia, R.H., Edgar, T.F., Rochelle, G.T., 2013. Two-stage flash for CO₂ regeneration: dynamic modeling and pilot plant validation. *Energy Procedia* 37, 2133–2144.
- Whyatt, G.A., Freeman, C.J., Zwoster, A., Heldebrant, D.J., 2016. Measuring nitrous oxide mass transfer into non-aqueous CO₂BOL CO₂ capture solvents. *Ind. Eng. Chem. Res.* 55, 4720–4725.
- Whyatt, G.A., Zwoster, A., Zheng, F., Perry, R.J., Wood, B.R., Spiry, I., Freeman, C.J., Heldebrant, D.J., 2017. Measuring CO₂ and N₂O mass transfer into GAP-1 CO₂-capture solvents at varied water loadings. *Ind. Eng. Chem. Res.* 56, 4830–4836.
- Xue, B., Yu, Y., Chen, J., Luo, Z., Wang, M., 2017. A comparative study of MEA and DEA for post-combustion CO₂ capture with different process configurations. *Int. J. Coal Sci. Technol.* 4, 15–24.
- Zhang, Q., Turton, R., Bhattacharyya, D., 2016. Development of model and model-predictive control of an MEA-based Postcombustion CO₂ capture process. *Ind. Eng. Chem. Res.* 55, 1292–1308.
- Zheng, F., Heldebrant, D.J., Mathias, P.M., Koech, P.K., Bhakta, M., Freeman, C.J., Bearden, M., Zwoster, A., 2016. Bench-scale testing and process performance projections of CO₂ capture by CO₂-binding organic liquids (CO2BOLs) with and without polarity-swing-assisted regeneration. *Energy Fuels* 30 (2), 1192–1203.
- Zheng, R.F., Barpaga, D., Mathias, P.M., Malhotra, D., Koech, P.K., Jiang, Y., Bhakta, M., Lail, M., Rabindran, A.V.R., Whyatt, G.A., Freeman, C.J., Zwoster, A.J., Weitz, K.K., Heldebrant, D.J., 2020. A single-component water-lean post-combustion CO₂ capture solvent with exceptionally low operational heat and total costs of capture -comprehensive experimental and theoretical evaluation. submitted to Energy Environ. Sci.